



Wadi Ziqlab Revisited: Estimation of Soil Loss and Prioritization of a Mountainous Watershed (Northern Jordan) Using RUSLE and GIS

Samer Nawaiseh

Yarmouk University, Department of Geography, Irbid, Jordan.

(Corresponding author: Samer Nawaiseh)

(Received 23 October 2020, Revised 01 December 2020, Accepted 23 December 2020)

(Published by Research Trend, Website: www.researchtrend.net)

ABSTRACT: The current research aims to estimate the damage to the soil and prioritize 30 sub-watersheds connected to W. Zeklab in northern Jordan. Research has been carried out by integrating RUSLE models, GIS, and remote sensing techniques. The local distribution of soil loss risk is edited by combining RUSLE Factors (R, K, LS, C, and P) on a raster-based GIS platform using various data sources. The map of soil damage produced shows five categories about the intensity of soil damage: small (0.0-15 tons, Ha-1, Year-1), Medium (15-30 tons, Ha-1), High (30-70 tons, Ha-1 >) year-1). The estimated average annual soil loss is 46.757 tons. Ha-1. The year-1 and the possible loss rate from the decay category range from 0.0 to 1707 tons. Ha-1. Year 1. While the lower and upper water bodies dominate the scattered areas of the lower and lower level of the risk of small soil erosion, the high, very high, and very high loss risk can be differentiated in the middle and upper parts of the class. In addition, the main wadi course and steep valley side slopes represent heavy isolated denudal slopes. Thus, the W.G.C.B. basin is considered to be an area of extreme decay. Realizing that the potential acceptable limit for the Mediterranean region is estimated at 2 to 12 tons. Ha-1. Year-1, priority sub-soil identification is important, which is necessary to maintain old conservation structures from one hand to another in the 1960s and to build new soil conservation systems to cover water from the other. Such methods are significant in reducing the soil runoffs, peak flows, and flood scum and thus restoring the storage capacity of the wetlands. Thirty sub-divisions are preferred in four categories - low, medium, high, and very high risk of loss. High and very high priority sub-divisions are condensed between the middle and upper catchment. Soil loss rate and priority maps help in the formulation of soil conservation and watershed management plans for Dw. ZekalbAwas.

Keywords: Jordan; Soil Erosion; RUSLE; Prioritization; Mountainous Watershed; Wadi Ziqlab.

I. INTRODUCTION

Soil erosion is a major natural risk caused by physical and anthropological processes. This is a growing concern in developing countries around the world and developing countries, including Jordan. As a result, the degradation and reduction of soil is important due to the potential negative effects of water quality degradation, nutritional loss, waste in wetlands and reduction of soil productivity. To meet the appropriate soil and water conservation plans, high soil degradation areas must be identified, mapped, evaluated, and estimated average annual soil loss rates. The average annual soil loss rate worldwide is widely recorded [1] Annual average of 30 to 40 tons of soil damage is reported. Ha-1. Year-1 for Asia, South America and Africa [2] Reports that Asia is one of the highest soil erosion zones (74 tons AC-1. year-1). Soil erosion in India indicates that 1100 million hectares and 550 million hectares have been affected by water and wind damage respectively. An average of 17 tons. Ha-1. Year-1 for the United States and Europe. In contrast, the minimum soil damage rate is recorded for the undisturbed forest. Report rate 0.004 to 0.05 tons. ha-1. Year-1 globally ([4]. Likewise, Farhan and Nawaiseh reviewed soil erosion rates for eastern and western Mediterranean watersheds and concluded that the average annual soil loss ranges from 1.0 to 205.47 tons. ha-1. year-1, whereas the mean values vary for different watersheds in Central and Northern Jordan.

For example, a mean value of 64 tons. ha-1. year-1 was estimated for W. Kerak [5]; 10 tons. ha-1. year-1 for W. Kufanja [6]; and 46.757 tons. ha-1. year-1 for W. Ziqlab [7]. Based on the type of erosion processes, different types of soil erosion predominate the northern highlands of Jordan, such as sheet erosion created by un-concentrated flow; rill and gully erosion (0.5 m and 1-3 m of depth respectively), developed by concentrated flow, inter-rill erosion as a result of raindrop impact on the soil surface (splash erosion), and overland flow in Jordan. Repetitive shallow and deep landslides also contribute significantly to soil erosion in the rejuvenated zone of the highlands [8]. Different models were developed to predict soil erosion loss at a watershed scale. Among these models are the physical-based models, i. e, Agricultural Nonpoint Source (AGNPS) [9], and Water Erosion Prediction Project (WEPP) [10]. European Soil Erosion Model (Morgan *et al.*,1998). Other models are empirical, i.e., the Universal Soil Loss Equation (USLE) [11], Revised Universal Soil Loss Equation (RUSLE) [12]. The MUSLE is an extension model for Universal Soil Loss Equation (USLE) [13]; designated to work at the finer temporal resolution, using peak flow and runoff to estimate event-based soil loss [14, 15]. The RUSLE is the most utilized model worldwide[16-27]. However, the application of the RUSLE model has been extended beyond soil loss estimation. Combined with the Sediment Supply Ratio

(SDR), this model was used to assess the life expectancy of semi-arid reservoirs, dams in Turkey [2, 29]. Lands have a higher risk of erosion than other land use/cover types. It is argued that soil erosion is intensifying in the medium and steep slopes that were converted to agricultural land; either with poor or excluded from soil conservation measures. Further, it is found that the major significant triggering factor for extreme soil erosion, landslide activity, and floods are the recurrent heavy rainstorms over the highlands of Jordan, with maximum daily intensity in the range of 2.2 – 6.6 mm hr⁻¹. Likewise, the RUSLE model has been employed. Landslides are possible in the northern part of the Greek island of Yubaoa due to soil erosion [30]. Furthermore, a satisfactory agreement was identified between the intensity of soil erosion zones and land sharing. [In this context they compared the local distribution of landslides to soil depletion risk zones and verified soil erosion in W. Kerra (high, very high and very high). A notable consistency was found between landslide distribution and high soil erosion zones. A similar conclusion was achieved by EbrahimZadehet al [31]. They reported that the distribution of large landslides in the Nozhian basin (Western Iran) is consistent with areas that had high erosion rates based on the RUSLE results. Such conclusions confirm that one of the dominant types of erosion in the Nozhian (Iran) and W. Kerak (Jordan) watersheds is landslide erosion.

Recently, [32] employed the RUSLE results in combination with morphometric analysis to prioritize thirty-one 3rd order sub-basins connected to W. Kerak (Central Jordan) using GIS. Similarly, [33] estimated soil loss to prioritize the sub-watersheds of Kali River catchment using the RUSLE approach, remote sensing, and GIS techniques. The RUSLE model has been employed to estimate soil loss for different catchments in the Central and Northern Highlands of Jordan. Original LULC Basically a spatial distribution map of rainwater harvesting, irrigation agriculture, rangeland and scattered forest remnants, arid Mediterranean, semi-arid and arid climate conditions under local soil distribution is possible and available at a reasonable cost. It provides accurate accuracy for water and regional scales for estimating soil erosion in three separate parts of the northern Jordanian highlands. Similarly w. Kufanja Catchment (North Jordan) employs Russell model to predict soil erosion. Previously acquired soil loss results were compared in North Jordan [38], and W. Crack watershed, and w. Along with other studies by Allarab Catchment [39], which indicates a steady decline in soil fertility and productivity.

Current research prioritizes OGKLB over soil loss estimates and 30 sub-basins using alligator models, gas and remote sensing techniques. Also, it is aimed to assess soil erosion status in the catchment with respect to soil conservation measures installed between 1965 and 1968 in the upper W. Ziqlab based on the descriptive survey carried out during the early sixties [7]. Due to development activities have taken place in northern Jordan since the 1970s, the retained results on soil erosion are significant for extending soil conservation measures to restore the watershed, and reduce soil erosion; thus, in turn, reducing the impact of drought and the possibility of flooding downstream.

II. THE STUDY AREA

W. Jikalb Falls 106 km². The range of latitudinal and length of the basin is 32° 25' N to 32° 31' N and 35° 30' E to 35° 49' E (Fig 1). It is located on the left bank of the Jordan River and is located in the northwest highland of Azlun, 80 km north of the capital Amman [7]. The minimum and maximum height of the waterfall - 228 meters above sea level and 1,068 meters above sea level (Fig. 2) is only 28 km. The upper catchment is composed of a completely divided morphology, smooth convex interfluvium and clean extraction extract form. Progressive revival in the upper, middle, and lower regions creates narrow and steep side-by-side girdles (30° - 40° and > 40°, Fig. 3) and valleys. W. G.G.B.'s Hypsometric Integral (HI) high (0.86) indicates that high total runoffs with the surface process form the most significant geologic process. Therefore, the loss of the basin, the induced channel incision, and the process of landslides in the specified sub-division [40] are considered high probability. The presence of deep and deep landslides indicates the past landslides, perhaps in the Pleocene and Quaternary era (< 5Ma) [41]. The upper Cretaceous marly clay and marly limestone of Ajlune group prevailed the catchment, and closely affects the soils of the basin. Vertisolic (cracking soils), typical Xerochrepts, Chromoxererts, and lithic soils cover the largest area in the watershed [42], while other types comprise alluvial wadi infill, variable soil types on slopes, and alluvial fan soils at the lower parts of W. Ziqlab at the base of the denudational fault-scarp overlooking the river Jordan. The horizon of the upper soil is wide, thus, the progressive decay on their surface reveals a more weakly formed sub-soil, which accelerates further decay [44, 7]. Dry Mediterranean climate dominates the upper part of the catchment with an average rainfall of 545 mm/year; And in the lower part, half-dry and dry, with annual rainfall of 420 and 300 mm/year respectively. About 80% of the annual rainfall falls between December and March. After years of snowfall, the most powerful source of rainfall. Related to soil erosion, the intensity of rainfall is more important than the annual rainfall. Most weather stations in W. Jikalb record 30-50 rain days [44] a year. However, the maximum 2.1 - 6.66 mm hour⁻¹ with severe storm normal [45, 46]. So the soil is a loss. The potential stream will change from 2050 mm/year to east [47] 2200 mm/year. The type of land cover is mainly covered in evergreen oak (*Quercus agrifolia*), irregular Aleppo pine (*Pinus halepensis*) and diagnostic oak (*Quercus aegilops*) [7] the upper and wettest eastern part and 30% of the basin is covered. Where 70% of the crops are land and rangeland. In 1966 the Jikalb Dam was built with 4.4 MCM [48] conservation capacity, and the irrigation was planned for agricultural purposes. Several springs are found across W. Jikalb through annual 5 MCM/Year Discharge [49]. However, Wadi is an additional 5 MCM/year flood water extraction in winter and spring [50].

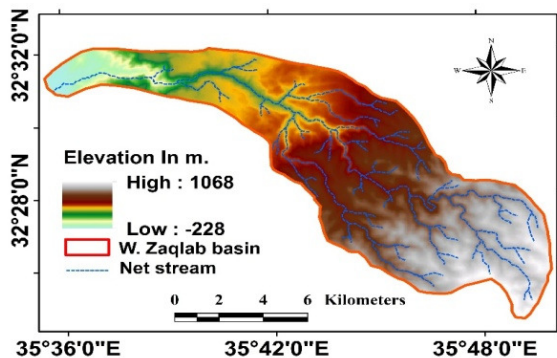


Fig. 1 & 2. The study area. The DEM of Wadi Ziqlab.

III. MATERIALS AND METHODS

A. Delineation of drainage and data used

For estimating soil erosion loss, the RUSLE model requires varied thematic layers as an input to assess soil erosion rates. These inputs are often extracted from various sources, i.e. remote sensing satellite data, topographic data, soil data, climatic, and field observations of available soil conservation measures. The methodology adopted to predict soil erosion loss over the W. Ziqlab watershed is displayed in (Fig. 3). Topographic maps (scale 1:50,000) of the Royal Jordanian Geographic Center (Amman) covering Wadi Ziqlab; were scanned, geo-referenced, and transformed to a zone 36 N projection system using Arc GIS 10.5. The entire catchment and 30 sub-basins were delineated initially using topographic sheets. ASTER DEM of 30 m resolution was utilized to demarcate the basin boundaries, and to extract the drainage network, and to generate topographic information for computing the RUSLE topographic factor [51] using Mitasova *et al.* [52] method. Further, to compile slope (degrees), elevation (m), flow direction, and flow accumulation maps, the Wadi Ziqlab watershed is classified as a sixth-order catchment, whereas the extracted 30 sub-basins are of second-order. Stream order was designated according to the ordering system elaborated by Horton [53] and Strahler [54]. LANDSAT 8 OLI (December 17, 2018) was subjected to supervised classification using Envi (4.5) and the Maximum Likelihood method, to classify land use/cover and to generate the LULC map. Soil texture data and other soil properties were acquired from the National Soil and Land Use Survey maps and reports [55]. Rainfall data for eight weather stations distributed over and close the catchment; were obtained from the Ministry of Water and Irrigation (Amman) with rainfall average ranges from 30 to >40 years, and were employed to compute R values. In the present study, the C factor was determined from the NDVI interpreted using image data from LANDSAT OLI, and the spatial distribution of the C factor was computed. P-values were assigned based on the derived LULC map from the LANDSAT image, and the corresponding slope class in each LULC type [34].

B. Methodology

The RUSLE approaches

RUSLE is an experienced soil loss model that is assigned to estimate the average annual loss caused by annual average soil loss and reel loss [34, 12]. Using RUSLE methods, average annual soil loss can be

predicted under various conditions of crop system, land management conditions, and loss control exercises. So the RUSLE model is created to guide soil conservation plans to control soil erosion. Whatever the limitations and the recent limitations described by Benavidez *et al.*, the model is the most widely employed experimental model for estimating soil damage, because of this flexibility, time, and cost-effective, and can be adopted in regions of scarce measured data, thus it can be utilized for watershed conservation and management [56]. By combining GIS techniques, the soil is predicted on a cell-by-cell basis. 30 meters × 30 meters of grid cells are determined before calculating the environmental characteristics of these cells such as land use, soil type, and shields that affect the content of soil loss in various water cells. This kind of process is enough to establish a unique spatial analysis environment for GIS modeling [35, 57, 58, 56]. The RUSLE model developed as an equation which accommodates the main factors that control interrill and rill erosion such as climate (rainfall erosivity), morphology (slope length and slope steepness), soil characteristics (soil erodibility), vegetation, and land use/land cover (cover management practice), and erosion control practice. The RUSLE model is expressed as:

$$A = R \times K \times LS \times C \times P \quad (1)$$

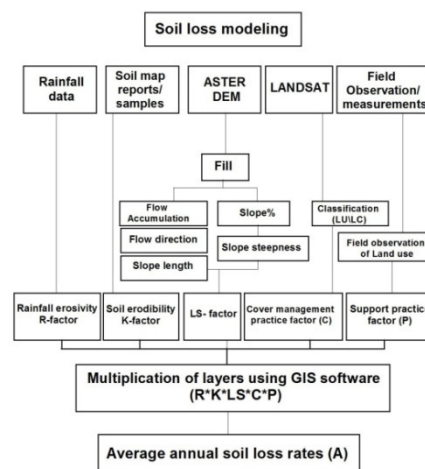


Fig. 3. Methodology adopted in the present study.

where A is the average annual soil loss ($\text{ton ha}^{-1} \text{yr}^{-1}$); R represents the rainfall-runoff erosivity factor ($\text{MJ mm ha}^{-1} \text{hr}^{-1} \text{yr}^{-1}$); K is the soil erodibility factor (soil loss per erosion index unit for a specified soil measured on a standard plot of 22.1 m long, 1.83m wide, and has a uniform slope of 5.6° [$\text{ton}^{-1} \text{ha}^{-1} \text{hr}^{-1} \text{ha}^1 \text{MJ}^{-1} \text{mm}^{-1}$] [59]. LS indicate the slope length and slope steepness factor (dimensionless); C is the cover and cropping management factor (dimensionless); and P implies the supporting practices factor, (ratio of soil loss with a support practice (i.e., contour tillage, strip-cropping, and terracing) to soil loss with row tillage parallel to the slope (dimensionless)).

Rainfall-runoff erosivity factor (R)

R Factor is a measure of local average annual rainfall and the loss of runoff steam that causes the intreeel and reel soil to be damaged. R value volume, intensity, duration, rainfall pattern (for single or storm events) and results are largely influenced by the amount and rate of

the runoff. High rainfall accelerates the intensity and duration of the precipitation and increases the R quality. The loss of rainfall is also affected by the slope standing. The area with high slope degrees has a greater erosion than the lower slope degrees. The R value can be extracted from the isoerodent map, or obtained from the official record, or the historical data can be calculated from [12]. The data on rainfall from 30 to > 40 years average 40 years average 40 years is used to calculate The R value using the [60] equation based on the original equation developed for USLE and Russell Model. The detailed equation was tested in the northern highlands of Jordan, including the eastern part of W. Jikalb. R Factor is calculated using the following equations:

$$R = 23.61 \times e^{(0.0048p)} \quad (2)$$

Where p is the mean annual precipitation. Using the inverse distance weighted (IDW) interpolation technique, the raster map of rainfall erosivity (R factor) was generated. The average annual R factor values achieved for six stations illustrated in Table 1. The rainfall erosivity factor (R) for the six weather stations was found to be in the range of 168.84 and 290.33 MJ·mm·ha⁻¹·hr⁻¹·year⁻¹. The distribution of R values is assumed to be varied and consistent with the annual distribution of precipitation across the catchment. The highest R values (196.57–290.33 MJ·mm·ha⁻¹·hr⁻¹·year⁻¹) dominate the upper humid zones of the watershed, and the lowest (169.67 – 142.93 MJ·mm·ha⁻¹·hr⁻¹·year⁻¹) occurs in the semi-arid middle; and arid lower catchment. The influence of rainfall on soil erosion is high at the upper catchment with erosivity values range from 180 to 300 approximately. Fig. 4 reveals that R values increase from the arid catchment mouth in the west to the humid highlands in the east depending on the climate and rainfall characteristics.

Table 1: Rainfall-runoff erosivity factor (R values).

Station	P (mm)	R (MJ mm ha ⁻¹ h ⁻¹ year ⁻¹)
Deir Abi Said	459	168.84
Gumaim	460	169.67
Rihaba	556	271.58
W. Ziqlab	425	142.93
Orjan	570	290.33
Tayba	465	196.57

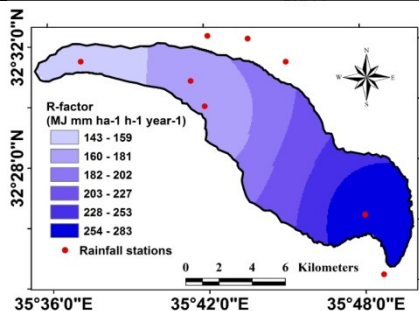


Fig. 4. Spatial distribution of rainfall erosivity (R) factor.

Oil erodibility factor (K)
The soil damage factor (K) represents the rate of soil loss, and the runoff amount produced by transport under a storm accident and rate, is measured under an ideal plot. Soil loss is assessed on scale 0 to 1, soil damage

(62), i.e., crop size distribution (% dirt, 0.002-01 mm), % organic matter indicates soil soil with the minimum probability of soil sample, soil formation, and permeability K factor 0 soil. The soil loss factor (K) is mainly represented by soil damage which is the RUSLE unit plot, which is 22.1 meters long, 1.83 meters wide, and has a shield of 5.6 s [58]. Factors (K) are calculated using the following equations developed by Wissmeier and Smith [34] and Renard etc.:

$$K = 27.66 m^{1.14} \times 10^{-8} \times (12 - a) + 0.0043 \times (b - 2) + 0.0033 \times (c - 3) \quad (3)$$

Where:

K= Soil erodibility factor (ton·hr⁻¹·ha⁻¹·MJ·mm).

m= (Silt% + Sand%) × (100 – clay%).

a= % organic matter.

b= structure code: 1) very structured or particulate, 2) fairly structured, 3) slightly structured, and 4) solid.

c= profile permeability code: 1) rapid, 2) moderated to rapid, 3) moderate, 4) moderate to slow, 5) slow, 6) very slow.

K Factor is also calculated using soil loss 'nomograph' method [65][34] in combination with soil properties (i.e., clay, sand, Dirt, and very fine sand, organic matter, soil structure, and permicity) which has been derived from the National Soil Map and Land Use Project[55]. Six different soil types exist in the W. Ziqlab catchment, the major soils are Xerochrepts, Chromoxererts, and Helplexerolls [43]. The dominant textural types are silty clay, silty loam, and silty clay loam with slight variation in CaCo3(%) and organic matter(%) (Table 2). It is obvious that the silty soils of the W. Ziqlab are expected to be of high erodibility, considering that the least resistant particles against erosion are silt and fine sand [56]. At present, recurrent drought events and human interventions, and misuse of the land have reduced vegetation cover in the eastern part of the Ziqlab catchment, thus rills and gullies are formed. Further, the soil of the eastern catchment area is mostly calcareous [66] with low nutrient availability. High silt content normally leads to unfavorable soil properties in terms of structure and crusting and impede plant growth, thus, in turn accelerating soil erosion. Applying the K- factor equation (3) and A digital map of BIS soil properties is applied using the inverse distance weight (IPW) interpolation method. Then, a map of a vector earth is converted to a raster format using the Spatial Analyzer tool. The soil layer value field was reclassified by K factor relative values using the Archival Special Analyst Extension redesign tool. As a result, the roster level of K-factor was established. Considering the different properties of the soil (e.g., structure, organic matter and differences) is achieved and a soil loss map is compiled [67]. Table 2 and Fig. (5) reveal that the K values of the soils vary from 0.0 24 to 0.34 (tons. ha. h. ha⁻¹. MJ⁻¹. mm⁻¹) for silty clay soils, and 0.041(tons. ha. h. ha⁻¹. MJ⁻¹.mm⁻¹). Regarding the classification of soil resistance to erosion; elaborated by Bollinne and Rosseau [68] based on the K-factor, it shows that 71.4% of the W. Ziqlab catchment is sensitive to erosion, while the rest of the catchment (28.6% of the area) is classified erosion-resistant soils (Table 3). This high erodibility is attributed to the silty loamy clay texture that dominated the watershed.

Table 2: Soil erodibility factor (K) values for various soil unit.

Soil texture	CaCo ₃ (%)	Organicmatter (%)	Soilerodibility factor(K) values (tonhahha ⁻¹ MJ ⁻¹ mm ⁻¹)
Silty clay	23.0	1.4	0.024
Silty clay	29.0	1.3	0.033
Silty loam	25.3	1.4	0.034
Silty clay loam	20.8	1.3	0.041
Silty clay	13.9	1.2	0.024
Silty clay	23.0	1.4	0.024

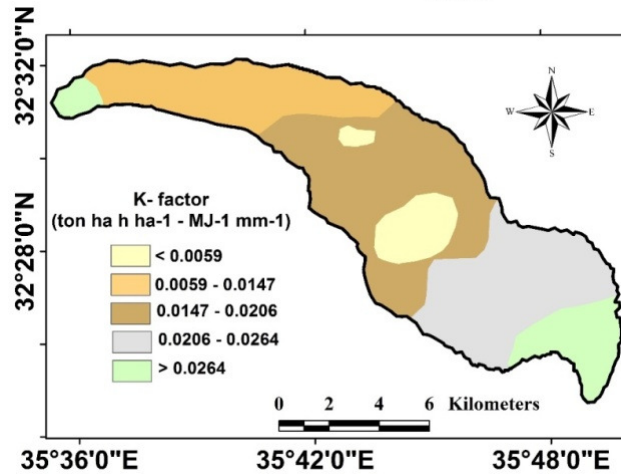


Fig. 5. Spatial distribution of soil erodibility factor (K).

Table 3: Classification of soil resistance of W. Ziqlab according to Bollinne and Rosseau (1978).

Erodibility	Erodibility (m)	Classification	Area	
			ha	%
< 0.01	< 0.0059	Very resistant to erosion	787.55	7.41
0.10 – 0.25	0.0059 – 0.0147	Resistant to erosion	2247.79	21.15
0.25 – 0.35	0.0147 – 0.0206	Moderate resistant to erosion	3568.29	33.58
0.35 – 0.45	0.0206 – 0.0264	Sensitive to erosion	2811.04	26.46
> 0.45	> 0.0264	Very sensitive to erosion	1209.46	11.38

Slope length and steepness factor (LS)

The topography effect on soil erosion is represented by the combined effect of slope length (L) and slope steepness (S) on erosion of slides, reefs and sheets. Operation length (L) and slope steepness (S) are the morphological parameters that affect soil erosion small erosion erosion, thus the Russell model [18] is responsible for the LS-factor. Russell's Topographic Factor (LS) represents a certain operation length and an operation constant [33] soil loss ratio. (L) Parameter means the ratio of internal reel loss (rain effect) to reel loss (developed by overland flow) to detect soil erosion associated with the ideal plot length of 22.1 m, or runoff focusing on a specific channel. Operation Vertical Parameters (S) 5.16 are related to the operational gradient loss effect compared to the standard plot vertical. The vertical effect of slope is greater on the erosion than the length of the rod. Consequently, the (LS) factor is considered to be 22.1 m long, 5.16 s as the predicted ratio of soil loss per unit, otherwise in the same situation. The 30 m resolution is adopted to achieve the Aster GDEM operation length and operation stability. In the present investigation, the combined operation length and slope steepness factor (LS) are calculated using the following equations described by Moore and Birch [71, 72].

$$LS = (\text{flow accumulation} \times \text{cell size} / 22.1)^{0.4} \times (\sin \text{slope} / 0.0896)^{1.3} \quad (4)$$

Where:

LS = the combined slope length and slope steepness factor. Flow storage indicates a given storage slope contribution area for a given cell, cell size means the size of the grid (30 meters in current research), and the sign shield degree shield angle is nothing but. The Arc GIS's spatial analyst tool is used to create a raster level of gradients, and from the hydrology tool, the flow direction and flow storage are calculated. The GIS raster calculator interface is inserted to compile the LS Factor map based on previous equations then the output level. LS factor values range from low (0.0) to high (321.5). Low LS values are connected to the lower slopes (5 s-10 s) and the medium slope (10 s-20 s) area (10 s-20 s) above and the rest of the waterfall and undulating summit (remnants of the lost surface) and the reef/fan basin of WG. High LS values stand, very steep, and highly steep slopes (10 - 15, 15, 20, 20, 30 and > 30) feature; Which is narrow, intense and vertical sideby, and widely divided into high and mid-catchment topography.

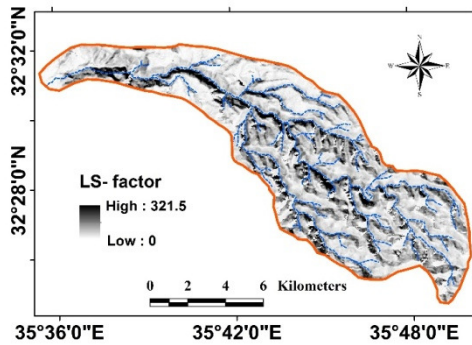


Fig. 6. Spatial distribution of LS factor.

Crop management factor (C)

The cover and management factor (C) is defined as the ratio of soil loss under specific cropping conditions to soil loss occurring in bare soil [34, 73]. The C-factor as the second substantial erosion factor following topography is remarkably influenced by human practices and efforts to reduce soil erosion. Consequently, the C-factor attribute explains the impact of cropping and other management practices on soil loss rates. C-values vary from 0.0 to 1.0 (no cover or a bare fallow land) [74]. Reported C-values for similar land cover related to other studies and carried out in the same area or region can be consulted to derive the C-factor values. At present, remote sensing-based classification techniques [35] are employed to classify land use/land cover (LULC), and the corresponding C-factor values for LULC classes can be achieved from the USLE guide tables developed by [34] or from reported literature and other similar case studies. In the present study, the LANDSAT OLI image was acquired for December 17 2018 (30 m resolution) and a land use/land cover map was produced using supervised classification; the Maximum Likelihood method and field inspection was performed to verify the results of the classification. Subsequently, C-factor values were determined from the Normalized Differential Vegetation Index (NDVI) values for soil loss assessment with RUSLE [75]. C-factor was computed using the following equation [76]:

$$C = \exp \left[-\alpha \frac{NDVI}{(\beta - NDVI)} \right]$$

Where α and β are the parameters that determine the shape of the NDVI–C curve and the C factor. An α value of 2 and β value of 1 was taken and affords rational results [76]. The relationship between C and NDVI values was established (Table 4) as $C = -0.619 X + 0.504$ ($R^2 = 0.985$), where the C-values in each land cell can be specified. The C-factor values in W. Ziqlab catchment range from 0.31 to 0.91 (Fig. 7). The highest C values (0.53) almost coincide with the NDVI values (-0.01) since the scattered forest of W. Ziqlab protects the soil against soil erosion, whereas the rangeland exposed to plowing has high C-values (0.35–40). Similarly, the mixed rainfed and irrigated farming areas have a C-value of 0.34 and 0.22 respectively. The model displayed logical results with a trend of increasing erosion with decreasing vegetation cover. Fig. 8 shows that low NDVI values are found mainly in the middle and lower parts of the catchment. Here urban areas overlapping with rainfed and irrigated farming, and

rangeland. However, although the upper part of the catchment is partially forested with scattered woods since late sixties, high C factor values are present. Overgrazing and wood cutting in the last two decades (following the rise of oil prices) make these areas more vulnerable to soil erosion.

Table 4: NDVI and C-factor values for different land cover types.

Landuse/covers	NDVI-Values	C-values
Barren lands	-0.01	0.53
Forest areas	0.60	0.13
Irrigated farming	0.40	0.22
Rainfed farming	0.20	0.34

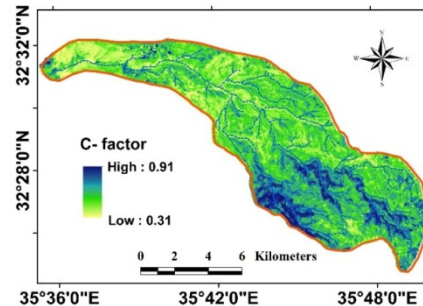


Fig. 7. Spatial distribution of C-factor values.

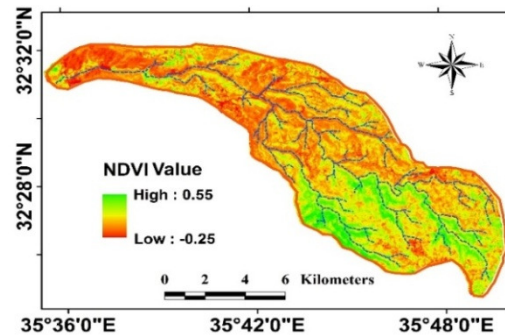


Fig. 8. Spatial distribution of NDVI values.

Conservation support practice factor (P)

Conservation Support Practice Factor (P) is defined as the ratio of soil damage to the soil after implementing a conservation exercise for soil damage directly on the top and for the lower slopes, and is used to understand conservation practices in the research area. P-Factor quality support practice is classified into agricultural land and other land use types [34]. P-factor is the RUSLE model depicts the effect of conservation practices that reduce the amount and rate of runoff, thus, in turn, minimizing soil erosion [77] through the control of runoff with explicit practices (i.e., contour tillage, terraces, and strip cropping) which aim finally to modify the pattern, direction, and speed of that runoff [12]. The lower the P-value the more effective the conservation practice is at mitigating soil erosion [1]. Nevertheless, the P-value varies from 0.0 to 1.0. If a value approaching 0.0, it indicates a good support practice available, whereas a value close to 1.0 refers to poor conservation practice [78]. A high P-value indicates a high soil erosion rate and vice versa. Field observations and visual image interpretation are proved to be useful in assessing

agricultural management practices. Aerial photos and Google Earth images also provide a high level of spatial details for visual assessment of the P-factor [79]. In the present study, P-values were assigned based on the derived LULC map from the appropriate LANDSAT image, and the corresponding slope class each LULC type [34]. Furthermore, Google Earth (2017), 1:25,000 air photos, and field inspection were utilized to arrive at a uniform P-factor value for the whole catchment. Tables elaborated by [80] the P factors for different types of agricultural management practices were also consulted. The structural conservation measures installed early in selected parts of the upper W. Ziqlab watershed (1965-1968), were not extended to other parts at a later stage as it should be [7]. Alternatively, 40-50% of the catchment lacks conservation practices, and the only support practice that exists is poor old terraces especially where rainfed farming including olive farming is practiced. Further, upslope and downslope tillage associated with poor conservation measures is still practiced as well. Irrespective that P-factor was assigned a value of 0.55 by the RUSLE [34, 12], and 0.6 for the rural tarmac roads, large areas without conservation measures were ascribed a P-factor value equal to 1.0. However, a uniform value of 0.8 was assigned for the W. Ziqlab catchment as proposed by other researchers who conducted similar research in the Mediterranean environment [81, 64, 82, 6]. Table 5 and Fig. 8 show that the value of P-factor varies from 0.45 to 0.99, in which the highest value is connected to areas with a shortage or no conservation practices. These areas also corresponding to steep, very steep, and extremely steep slope categories while the lowest values are assigned to agricultural land generally.

Table 5: Support practice factor (P).

Land use type	Slope (°)	P factor
Agriculture	0 – 6	0.45
	6 – 20	0.65
	20 – 30	0.74
	30 – 40	0.81
Other land	All	0.99

IV. RESULTS AND DISCUSSION

Estimation of average annual soil loss

The average annual soil loss values vary from 0.0 to 1707 ton. ha⁻¹. year⁻¹ (Fig. 9). year⁻¹, with a mean value of 46.757 ton. ha⁻¹. year⁻¹. The watershed was classified into five rates of erosion risk classes (ton. ha⁻¹. year⁻¹): slight (0-15), moderate (15-30), high (30-70), very high (70-80), and extremely high > 180). Maximum soil damage is combined with mixed rain and irrigation cultivation on both small slopes. (0-5° and 5-10°), and steep sloping land (15-20°, 20-30°, and > 30°), rangeland, bare land, and steep slopes characterize the dissected denudational slopes in the south and southeast parts of the catchment. Overgrazing in the past and present, along with the continuous cutting of scattered forest are as accelerate soil erosion in the southeastern part of the basin. Table 6 and Fig. 10 show that 39.564% of the W. Ziqlab basin counters soil erosion between 0.0 to 30 tons. ha⁻¹. year⁻¹ (slight and moderate soil erosion risk), whereas 60.4362% of the watershed area predicted to have soil erosion rates

range from 30 to > 180 ton. ha⁻¹. year⁻¹ (high, very high, and severe erosion risk). However, extremely high soil erosion risk occurs across the gorge-like nature along the main wadi course and major tributaries. The slight and moderate erosion risk is restricted to gentle/undulating slopes occupy the interfluvial and the lower rift floor and fan of W. Ziqlab. Slight soil erosion risk (0-15 ton. ha⁻¹. year⁻¹) is estimate only 24.1% of the study catchment. By contrast, 12.909% of the watershed is estimated to suffer extremely high erosion risk with soil loss greater than 180 tons. ha⁻¹. year⁻¹. By contrast, 12.909% of the watershed is estimated to suffer extremely high erosion risk with soil loss greater than 180 tons. ha⁻¹. year⁻¹.

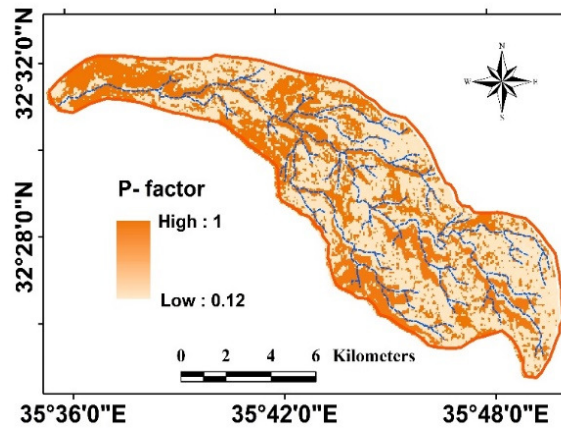


Fig. 9. Spatial distribution of P factor.

Table 6: Soil erosion loss categories.

Soil loss category	(ton. ha ⁻¹ . year ⁻¹)	Area (km ²)	Area (%)
Slight	0.0 to 15	26.51	24.10
Moderate	15 to 30	17.01	15.464
High	30 to 70	30.02	27.2909
Very high	70 to 180	22.26	20.2363
Extremely high	> 180	14.20	12.909

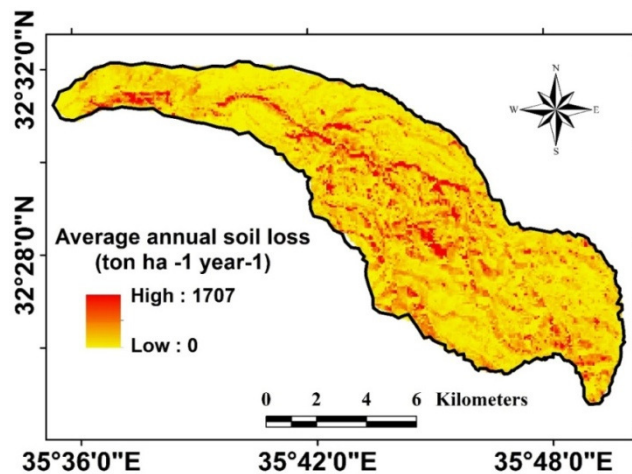


Fig. 10. Spatial distribution of average annual soil loss (ton·ha⁻¹·year⁻¹).

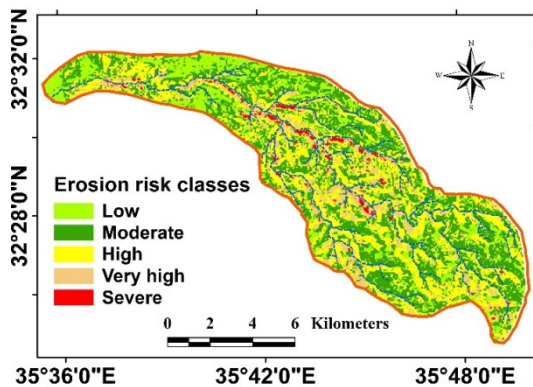


Fig. 11. Soil erosion risk classes.

The validation of RUSLE results

The estimated annual soil loss of W. Ziqlab (46.7 ton. ha⁻¹. year⁻¹) is inconsistent with values achieved for neighboring rift watersheds (Table 7) irrespective of the

Table 7: Comparison of soil loss estimation in central and northern rift watersheds.

Study watershed/area	Mean annual Rainfall(mm)*	Mean average annual soil loss (ton. ha ⁻¹ . Year ⁻¹)	Reference
W. Kufranja	<100 – 200 mm in the rift floor and northern Badia to	10	Farhan <i>et al.</i> 2013
Mafraq - Irbid area, northern Badia		9.53	Alkharabsheh <i>et al.</i> 2013
W. Kerak	640 mm	64	Farhan and Nawaiseh 2015
W. Alarab	in the northern	32.5	Farhan and Nawaiseh 2019
W. Ziqlab-the present study	highlands	46.7	Nawaiseh and Farhan 2019

*Source: Farhan and Alnawaiseh(2018) [38]

The spatial correlation of soil erosion intensity and landslide distribution in W. Kerak shows that a high erosion zone has a higher probability of landslide events [5]. The northern rift watersheds including W.Ziqlab are characterized by large and small arcuate scars and hummocky topography indicates past landslide episodes, possibly of Pliocene and Quaternary age (< 5 Ma) [41, 42]. To verify this fact and its applicability to neighboring rift watersheds (including W.Ziqlab), the frequent ratio-based statistical analysis method developed by Pradhan *et al.*, (2012) was applied to confirm the relationship between landslide distribution and soil erosion intensity. The results reveal that a strong relationship exists between landslides and a given soil erosion loss zone, thus a high probability of the occurrence of slope failures across zones of high soil loss rates. Visual interpretation of air photos and field observations show that high soil erosion zones occurred in the middle and upper parts of the catchment. Consequently, it is expected that a satisfactory agreement exists between soil loss rates and the distribution of landslide events over W.Ziqlab and other comparable watersheds in the rift highland watersheds of Jordan. Hence, the RUSLE model can be applied for demarcating sites susceptible to landslides triggered by soil erosion. Recently, the Ziqlab reservoir has lost substantial storage capacity as a consequence of sediment infilling. The annual

higher estimated annual soil loss for W. Kerak (64 ton. ha⁻¹. year⁻¹) although greater rainfall (300 – 640 mm) is experienced in these areas. By contrast, the W. Ziqlab attains an estimated average annual soil loss at 46.7 tons. ha⁻¹. year⁻¹; whereas W. Alarab is found to be 32.5 tons. ha⁻¹. year⁻¹. The high rate of soil damage to W. Kera is evident from the impact of weak defensive land cover, old landslides, repeated deep and deep landslides, frequent co-operative faults that have been lost from the kera, and the significant increase in the average annual soil loss from the highlands exceeds the 2 to 12 tonne tolerance limit. Ha-1. Year-1 for Mediterranean Waters [83, 84, 81, 85]. Consequently, priority must be given to the protection of present vegetation cover, afforestation of bare-sloping lands, shallow landslide areas, the construction of appropriate conservation measures, and improving agricultural management practices to reduce erosivity effects of soil loss.

sediment rate has been estimated at 0.046 MCM, and the estimated sediments accumulated from 1966 to 2012 was exceeded 2 MCM [49], with slightly half of the reservoir gross storage capacity being lost due to sedimentation. It is worth to report that high rates of sediment estimation were achieved following the implementation of the W. Ziqlab conservation project in the 1960s. The previous research on soil erosion estimation over the northern rift watersheds, along with the consistent relationship established between landslide distribution and soil erosion intensity, and sedimentation estimation, represent direct evidence for the validation of the RUSLE results achieved for W. Ziqlab.

Prioritization of sub-watersheds

Prioritization of sub-watersheds entails the ranking of different sub-catchments in terms of the order they have considering the amount of soil loss, and to be chosen for appropriate soil conservation treatment. Adaptation of soil conservation measures priority-wise is aimed to reduce soil erosion loss, increase the availability of surface and groundwater, and in turn reduces the probability of droughts and flooding [86, 87, 33]. Using Arc GIS tools and ASTER DEM, 30 sub-basins of 2nd order were delineated (Fig. 12) in order to perform prioritization and to establish the spatial distribution of priority classes. Prioritization of sub-basins assigns to the "ranking of different sub-basins in relation to the order they have to be selected for suitable soil

conservation measures adaptation" [88]. The average annual soil loss of 30 sub-basin has been computed and displayed in Table (8). The highest average annual soil loss is found is connected to sub-basin No. 10. (165.91 ton. ha⁻¹. year⁻¹). Whereas the lowest average annual soil loss characterized sub-watershed No. 22 and yield 26.91 ton. ha⁻¹.year⁻¹. Based on the average annual soil loss, the 30 sub-basins have been prioritized into four priority classes: low < 35 ton. ha⁻¹. year⁻¹; moderate 35 – 75 ton. ha⁻¹. year⁻¹; high 75 – 120 ton. ha⁻¹. year⁻¹; and very high > 120 ton. ha⁻¹. year⁻¹. The highest priority for soil conservation adaptation is designated to the sub-basin having the highest soil loss. The highest priority denotes the great degree of soil erosion in a particular sub-watershed and needs immediate intervention to enhance available soil and water conservation, or, to install/expand additional soil conservation measures. Accordingly, such sub-basins are considered a potential area for applying soil conservation treatment [89]. Out of 30 sub-basins, 5 sub-catchments (16.7%) are ranked under very high priority (Fig. 13), as they have very high values of soil loss (> 120 ton. ha⁻¹. year⁻¹). These sub-basins (10, 15, 16, 25, and 27) occupy the core of the rejuvenated belt characterized by deeply incised channels and very steep slopes [90]. Ten sub-watersheds fall in the high – priority category (33.3%) with average annual soil loss values between 75 – 120 ton. ha⁻¹. year⁻¹. Without exception all these sub-watersheds are located in the middle and upper parts of W. Ziqlab (sub-basins 1, 2, 4, 6, 8, 13, 14, 17, 20, and 26). Very high and high priority classes constitute 50% of the watershed area. The igh soil loss rates in these sub-basins increase the sediment deposition downstream in W. Ziqlab dam. Consequently, the two priority classes need an immediate adaptation of soil conservation measures. Thirteen sub-basins are classified under moderate class (3, 5, 7, 9, 11, 12, 18, 19, 23, 24, 28, 29, and 30) and represent 43.3% of the total sub-basins. These sub-watersheds are distributed over the lower, middle, and upper parts of the watershed. Eight moderate priority sub-basins are located in areas covered by the forest remnants and the old soil conservation measures installed during 1965-1968. Two sub-basins have been placed under low priority class (21 and 22) and covering 6.7% of the total

sub-watersheds. These sub-basins are located downstream, with relatively low soil erosivity values (< 35 ton. ha⁻¹.year⁻¹), and the morphology is dominated by gentle/undulating sloping terrain and alluvial fan. Intensive exploitation of soil resources over the last 3000 years [91] has contributed to considerable destruction of vegetation cover, severe soil erosion, the continuous decline of crop yield and livestock, and the suffering of local farmers. Different conservation techniques have been adopted by the rainfed farmers since the Nabatean period, some 3000 years ago [91]. Renewal of some conservation techniques is recommended since local farmers are familiar with such techniques. On slopes ranging from 3 to 25 degrees, check dams, terracing, and bunding are proposed. Slope steepness is traditionally modified through the construction of contour stone terraces; accompanied by tree-planting [92]. Bench terraces can also be constructed on slopes greater than 25 when stones are not available to construct contour stone terraces. It is advised to integrate structural conservation solution with technology aiming to improve cropping system, i.e., rotation strip cropping, contour strip intercropping cultivation [93]. Moreover, rangeland management is required to protect the degraded vegetation cover, and redeveloping the natural vegetation through seeding with suitable grasses, expanding tree-planting of drought – resistance species, and planning for effective rangeland management [94].

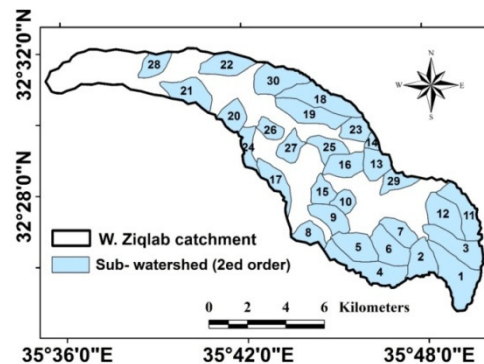


Fig. 12. The 30 sub-watersheds of W. Ziqlab.

Table 8: Average soil loss and priority classes of 30 sub-watersheds of W. Ziqlab.

Sub-basin no.	Average soil loss (t. ha ⁻¹ year ⁻¹)	Priority	Sub-basin no.	Average soil loss (t. ha ⁻¹ year ⁻¹)	Priority
1	117.61	High	16	164.69	Very high
2	118.87	High	17	86.01	High
3	65.11	Moderate	18	63.60	Moderate
4	84.64	High	19	51.10	Moderate
5	46.23	Moderate	20	101.33	High
6	76.35	High	21	32.70	Low
7	70.28	Moderate	22	26.91	Low
8	119.12	High	23	47.14	Moderate
9	64.38	Moderate	24	71.34	Moderate
10	165.91	Very high	25	137.58	Very high
11	72.55	Moderate	26	114.45	High
12	45.04	Moderate	27	134.42	Very high
13	104.43	High	28	52.95	Moderate
14	83.47	High	29	55.77	Moderate
15	125.11	Very high	30	36.17	Moderate

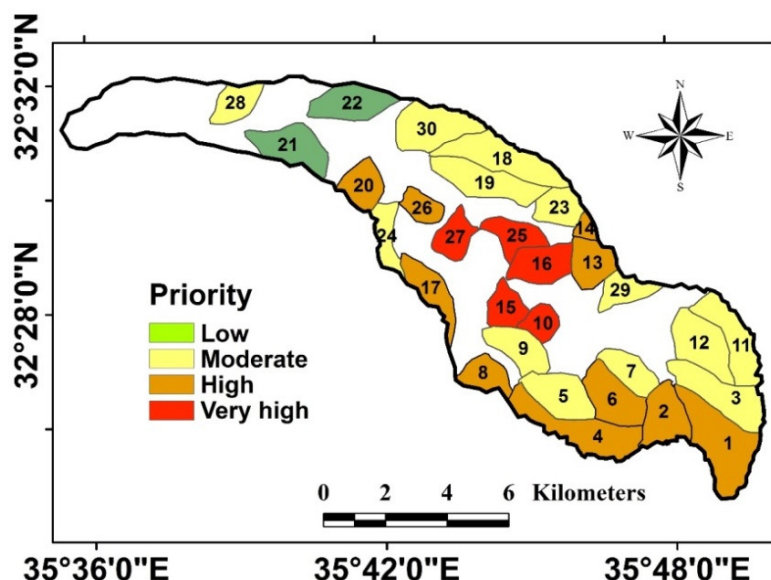


Fig. 13. Priority categories of 30 sub-watersheds of W. Ziqlab based on soil erosion.

V. CONCLUSION

The RUSLE – an empirical soil erosion model; was integrated with GIS to estimate the annual soil loss rate for the W. Ziqlab catchment. The associated 30 sub-watersheds were prioritized in four categories with different erosion risk levels. It is found that the RUSLE model effective for priority-wise soil conservation planning and watershed management. The average annual soil loss values vary from 0.0 to 1707 ton.ha⁻¹.year⁻¹, with a mean value of 46.757 ton.ha⁻¹.year⁻¹.out of the thirty sub-watersheds sub-basin No. 22 exhibits the lowest soil loss (26.91ton.ha⁻¹.year⁻¹), while sub-basin No. 10 yieldsthe maximum soil loss which is 165.91 ton.ha⁻¹.year⁻¹.Very high priority (soil loss was estimated at > 120 ton. ha⁻¹. year⁻¹) and high priority (soil loss values was estimated at 75 – 120 ton. ha⁻¹. year⁻¹) classes constitute 50% of the watershed area and located in the middle and upper of the W. Ziqlab watershed. The highest priority indicates that surface erosion rates are considerably high. Consequently, appropriate soil conservation measures must be taken immediately for very high and high priority classes to reduce runoff coefficient, increase infiltration rates and soil moisture in the soil profile, and in turn reduce sedimentation in the W. Ziqlab dam. High soil erosion rates estimated for sub-watersheds in the middle and upper catchment revealed that the conservation measures installed during the 1960s are not effective in reducing soil erosion. Further, the long periods of human intervention, land use abuse, the deterioration of vegetation cover and forest remnants in the last two decades;were decisive in maximizing soil erosion over the sub-watersheds which traditionally rainfed farming has been practiced, (or) rangeland transformed to rainfed"mixedfarming" since the 1950s. Sub-catchments classified as a high and moderate priority have experienced historically severe soil erosion rates, and occupy a considerable part of rainfed areas, overgrazed rangeland, destructed natural vegetation cover, and bare land. Nevertheless, the cultivated land with poor conservation measures exhibits a higher rate of soil erosion and decline in soil fertility. Therefore, all

sub-basins that fall under high and moderate priority are vulnerable to soil erosion, hence, they should be prioritized for conservation measures.Thestudy confirmed the role of the RUSLE model and GIS tools for soil loss estimation efficiently, exploring high erosion-prone areas, and priority classification. The results of the RUSLE prediction of soil erosion loss were validated regardingrecent soil loss estimation in comparable rift catchments in central and northern Jordan using the RUSLE approach. An investigation was carried out in the W. Kerakwatershed using consistent statistical techniques and intensive fieldwork; concluded that high soil erosion risk zones were concentrated within the rejuvenated belt; and on steep denudational slopes, Aspatial correlation also is well-founded between high soil erosion zones and large landslide zones. Thus, a high erosion zone has a higher probability of landslide events. In this regard, all the rift catchments in central and northern highlands are considered a high-risk landslide hazard zone. Old landslide complexes and recent deep and shallow landslides are often associated with severe soil erosion zones.However, further study on direct field measurements of soil erosion in W. Ziqlab, assessment of sediment yield/ deposition in W. Ziqlab dam, rangeland management, and proper land utilization; are prerequisites to reduce soil erosion hazardto maintain future farming sustainability.

ACKNOWLEDGEMENTS

This work was initially a joint research project with Professor Yahya Farhan, former University of Jordan, but God died before the research was over. I would like to express my great appreciation for his spirit, the mercy of God.

REFERENCES

- [1]. Bagherzadeh, A. (2014). Estimation of Soil Losses by USLE Model Using GIS at Mashhad Plain, Northeast of Iran. *Arabian Journal of Geosciences*, 7, 211-220.
- [2]. El-Swaify, S.A., & Dangler, E.W. (1976). Erodibilities of Selected Tropical Soils in Relation to Structural and Hydrologic Parameters, *Soil and Water Conservation Society*, Ankeny, Iowa.

- [3]. Saha, S.K. (2004). Water and Wind Induced Soil Erosion Assessment and Monitoring Using Remote Sensing and GIS. In: M.V.K. Sivakumar, P. S., Roy, K. Harmsen, & S.K. Saha (Eds.), *Satellite Remote Sensing and GIS Applications in Agricultural Meteorology*, Proceedings of a Training Workshop held 7-11 July 2003 in Dehra Dun, India, AGM-8, WMO/TD-No.1182, pp.315330
<http://www.wamis.org/agm/pubs/agm8/WMOTD1182.pdf>
- [4]. Pimentel, D., Harvey, C., Resosudarmo, P., Sinclair, K., Kurz, D., McNair, M., & Blair, R. (1995). Environmental and Economic Costs of Soil Erosion and Conservation Benefits, *Science*, 267, 1117-1123.
- [5]. Farhan, Y., & Nawaiseh, S. (2015). Spatial Assessment of Soil Erosion Risk Using RUSLE and GIS Techniques. *Environmental Earth Sciences*, 74, 4649-4669.
- [6]. Farhan, Y., Zerqat, D., & Farhan, I. (2013). Spatial Estimation of Soil Erosion Risk Using RUSLE Approach, RS, and GIS Techniques: A Case Study of Kufranja Watershed, Northern Jordan. *Journal of Water Resources and Protection*, 5, 1247-1261.
- [7]. Beaumont, P., & Atkinson, K. (1969). Soil Erosion and Conservation in Northern Jordan. *Journal of Soil and Water Conservation*, 24, 144-147.
- [8]. Al-Sherideh, M. S., Malkawi, A., Al-Hamdan, H., & Abdulrahman, N. (2000). Evaluating Sediment Yield at King Talal Reservoir from Landslides along Irbid-Amman Highway. *Engineering Geology*, 56, 361-342.
- [9]. Young, R. A., Onstad, C. A. Bosch, D. D., & Anderson, V. P. (1989). AGNPS - a Non-Point Source Pollution Model for Evaluating Agricultural Watersheds. *Journal of Soil and Water Conservation*, 44, 168-173.
- [10]. Foster, G. R., & Lane, L. J. (1987). User Requirements: USDA Water Erosion Prediction Project (WEPP). NSERL Report No.1. West Lafayette, Indiana: USDA ARS National Soil Erosion Research Laboratory.
- [11]. Wischmeier, W. H., & Smith, D. D. (1978). Predicting Rainfall Erosion Losses: A Guide to Conservation Planning. *USDA Handbook 537*, Washington D.C.
- [12]. Renard, K. G., Foster G. R., Weesies G. A., McCool D. K., Yoder D. C. (1997). Predicting soil erosion by water: a guide to conservation planning with the revised universal soil loss equation (RUSLE). *Agricultural handbook no. 703*. US Department of Agriculture, Agricultural Research Service, Washington, DC 404 pp.
- [13]. Williams, J. R. (1975) Sediment Yield Prediction with Universal Equation Using Runoff Energy Factor. In: Present and Prospective Technology for Predicting Sediment Yields and Sources. Agricultural Research Service, US Department of Agriculture, Washington DC, 244-252.
- [14]. Sadeghi, S. H. R., Gholami, L., Khaledi Darvishan, A., & Saeidi, P. (2014). A Review of the Application of the MUSLE Model Worldwide. *Hydrological Sciences Journal*, 59, 365-375.
- [15]. Benavidez, H. Jackson, B. Maxwell, D., & Norton, K. (2018). A Review of the (Revised) Universal Soil Loss Equation ((R)USLE): With a View to Increasing its Global Applicability and Improving Soil Loss Estimates. *Hydrology and Earth System Sciences*, 22, 6059-6086.
- [16]. Angima, S. D., Stott, D. E., O'Neill, M.K., Ong, C. K., & Weesies, G. A. (2003). Soil Erosion Prediction Using RUSLE for Central Kenyan Highland Conditions. *Agriculture, Ecosystem & Environment*, 97, 295-308.
- [17]. Wu, L., Long, T., Liu, X. and Mmereki, D. (2012). Simulation of Soil Loss Processes Based on Rainfall Runoff and the Time Factor of Governance in the Jialing River Watershed, China. *Environmental Monitoring and Assessment*, 184, 3731-3748.
- [18]. Prasannakumar, V., Vijith, H., Abinod, S., & Geetha, N. (2012). Estimation of soil erosion risk within a small mountainous sub-watershed in Kerala, India, using revised universal soil loss equation (RUSLE) and geo-information technology. *Geosciences Frontiers*, 3(2): 209–215.
- [19]. Chatterjee, S., Krishna, A. & Sharma, A. (2014). Geospatial Assessment of Soil Erosion Vulnerability at Watershed Level in Some Sections of the Upper Subarnarekha River Basin, Jharkhand. *Environmental Earth Sciences*, 71, 357-374.
- [20]. Gao, H. D., Li, Z. B. & Li, P. (2015). The Capacity of Soil Loss Control in the Loess Plateau Based on Soil Erosion Control Degree, *Acta Geographica Sinica*, 70, 1503-1515.
- [21]. Duarte, L., Teodoro, A. Gonçalves, J., Soares, D. & Cunha, M. (2016). Assessing Soil Erosion Risk Using RUSLE through a GIS Open Source Desktop and Web Application. *Environmental Monitoring and Assessment*, 188, 1-16.
- [22]. Gaubi, I., Chaabani, A., Ben Mammou, A., & Hamza, M. H. (2016) A GIS-Based Soil Erosion Prediction Using the Revised Universal Soil Loss Equation (RUSLE) (Lebna Watershed, Cap Bon, Tunisia), *Natural Hazards*, 86, 219-239.
- [23]. Abdo, H., & Salloum, J. (2017). Mapping the Soil Loss in Marqya Basin: Syria Using RUSLE Model in GIS and RS Techniques. *Environmental Earth Sciences*, 76, 114-126
- [24]. Sharma, T., & Singh, O. (2017). Soil Erosion Susceptibility Assessment through Geo-stastical Multivariate Approach in Panchkula District of Haryana, India. *Modeling Earth System Environment*, 3, 733-753.
- [25]. Wang, G., Yu, J., Shrestha, S., Ishidaira, H. & Takeuchi, K. (2010). Application of a Distributed Erosion Model for the Assessment of Spatial Erosion Patterns in the Lushi Catchment, China. *Environmental Earth Sciences*, 61, 787-797.
- [26]. Benchettouh, A., Kouri, L. & Jebari, S. (2017). Spatial estimation of soil erosion risk using RUSLE/GIS techniques and practices conservation suggested for reducing soil erosion in Wadi Mina watershed (northwest, Algeria). *Arab J Geosci* 10, 79.
- [27]. Richardson, C. and Amankwatia, K. (2019). Assessing Watershed Vulnerability in Bernalillo County, New Mexico Using GIS-Based Fuzzy Inference. *Journal of Water Resource and Protection*, 11, 99-121. doi: 10.4236/jwarp.2019.112007.
- [28]. Saygin, S. D., Ozcan, A. U., Basaran, M., Timur, O.B., Dolarslan, M., Yilman, F. E. & Erpul, G. (2014). The Combined RUSLE/SDR Approach Integrated with GIS and Geo-statistics to Estimate Annual Sediment Flux Rates in Semi-Arid Catchment, Turkey. *Environmental Earth Sciences*, 71, 1605-1618.
- [29]. Adhikary, P. P., Tiwari, S. P. Mandal, D. Lakaria., B. L., & Madhu, M. (2014). Geospatial Comparison of Four Models to Predict Soil Erodibility in a Semi-Arid Region of Central India. *Environmental Earth Sciences*, 72, 5049-50-62.

- [30]. Rozos, D., Skilodimou, H. D., Loupasakis, C., & Bathrellos, G. D. (2013). Application of the Revised Universal Soil Loss Equation Model on Landslide Prevention. An Example from N. Euboea (Evia) Island, Greece. *Environmental Earth Sciences*, 70, 3255-3266.
- [31]. Ebrahimzadeh, S., Motagh, V. Mahboub, F., & Harijani, F. M. (2018). An Improved RUSLE/SDR Model for the Evaluation of Soil Erosion. *Environmental Earth Sciences*, 77, 454.
- [32]. Farhan, Y., & Anaba, O. (2016). Watershed Prioritization Based on Morphometric Analysis and Soil Loss Modeling in Wadi Kerak (Southern Jordan) using GIS Techniques. *International Journal of Plant and Soil Science*, 10, 1-18.
- [33]. Markose, V. J., & Jayappa, K. S. (2016). Soil Loss Estimation and Prioritization of Sub-Watersheds of Kali River Basin, Karnataka, India, Using RUSLE and GIS. *Environmental Monitoring and Assessment*, 188, 225.
- [34]. Wischmeier, W. H., & Smith, D. D. (1978). Predicting Rainfall Erosion Losses: A Guide to Conservation Planning. USDA Handbook 537, Washington D.C.
- [35]. Millward, A., & Mersey, J. E. (1999). Adapting the RUSLE to Model Soil Erosion Potential in a Mountainous Tropical Watershed. *Catena*, 38, 109-129.
- [36]. Al-Zitawi, F. (2006). Using RUSLE in Prediction of Soil Loss for Selected Sites in North and North West of Jordan. MSc. thesis. *Jordan University of Science and Technology*, Irbid.
- [37]. Farhan, Y., Zerqat, D., & Farhan, I. (2013). Spatial Estimation of Soil Erosion Risk Using RUSLE Approach, RS, and GIS Techniques: A Case Study of Kufranja Watershed, Northern Jordan. *Journal of Water Resources and Protection*, 5, 1247-1261.
- [38]. Farhan, Y., & Alnawaiseh, S. (2018). Spatio-Temporal Variation in Rainfall Erosivity over Jordan Using Annual and Seasonal Precipitation. *Natural Resources*, 9, 242-267.
- [39]. Farhan, Y., & Nawaieh, S. (2019). Prioritization of W. Alarab Sub-Watersheds (North Jordan) for Conservation Measures Using RS, GIS, and Multi-Criteria Analysis. *Journal of Water Resource and Protection*, 11, 995-1023. doi: 10.4236/jwarp.2019.118059.
- [40]. Farhan, Y., Mousa, R., Dagara, A., & Shtaya, D. (2016). Regional Hypsometric Analysis of the Jordan Rift Drainage Basins (Jordan) Using Geographic Information System. *Open Journal of Geology*, 6, 1312-1343.
- [41]. Quennell, A. (1958). The Structure and Geomorphic Evolution of the Dead Sea Rift. *Quarterly Journal of the Geological Society*, 114, 1-24.
- [42]. Farhan, Y. (1986). Landslides in Central Jordan with Special Reference to the March 1983 Rainstorm. *Singapore Journal of Tropical Geography*, 7, 80-96.
- [43]. Sa'da, M., Al-Malabeh, A., & Al-Khede, S. (2011). GIS-Based Documentation and Geo-Environmental Assessment of W. Ziqlab, North Jordan: Natural and Cultural Resources. The 10th International Conference of Jordanian Geologists Association. *The 7th International Symposium on Middle East Geology*, 3-5 April, Amman Jordan.
- [44]. Fisher, W., Atkinson, K., Beaumont, P. Coles, A., & Gilchrist-Shirlaw, D. (1966). Soil Survey of WadiZeqlab, Jordan, University of Durham, Durham.
- [45]. Farhan, Y. (1999). Geomorphic Impacts of Highway Construction, Their Causes and Remedies: A Case Study from Aqaba, Southern Jordan. *Arab World Geographer*, 21-25.
- [46]. Farhan, Y. (2002). Slope Stability Problems in Central and Northern Jordan. *Arab World Geographer*, 5, 265-290.
- [47]. El-Radaideh, A., Al-Taani, A. Al-Momani, T., Tarawneh, K., Batayneh, A., & Taani, A. (2014). Evaluating the Potential of Sediments in Ziqlab Reservoir (Northwest Jordan) for Soil Replacement and Amendment. *Lake and Reservoir Management*, 30, 32-45.
- [48]. MacDonald, M. (1965). Wadi Ziqlab Dam. Geological Report on the Upper Dam Site, Ministry of Water and Irrigation, Amman, Jordan.
- [49]. Shatnawi, A. (2002). Hydrological and Hydrochemical Study for Zeglab Dam. MSc. thesis, Al al-Bayt University, Mafrqa.
- [50]. Water Authority of Jordan (WAJ). (1989). The North Jordan Water Resources Investigation Project.
- [51]. Oliveira, T. S., Rodrigues, P. B., Sobrinho, D. A. B., Panachuki, T. E., & Wendland, E. (2013). Use of SRTM Data to Calculate the (R) USLE Topographic Factor. *Acta Scientiarum-Technology*, 35, 507-513.
- [52]. Mitasova, H., Hofierka, J., Zlocha, M., & Iverson, R. (1996). Modeling Topographic Potential for Erosion and Deposition Using GIS. *International Journal of Geographic Information System*, 10, 629-641.
- [53]. Horton, R. (1945). Erosional Development of Streams and their Drainage Basins: Hydrological Approach to Quantitative Morphology. *Geological Society of America Bulletin*, 56, 275-370.
- [54]. Strahler, A. (1957). Quantitative Analysis of Watershed Geomorphology. *Transactions, American Geophysical Union*, 38, 913-920.
- [55]. Ministry of Agriculture Jordan (1995). The Soils of Jordan. Report of the National Soil Map and Land Use Project, Ministry of Agriculture, Hunting Technical Services Ltd. and European Commission, Amman.
- [56]. Prasannakumar, V., Shiny, R., Geetha, N., & Vijith, H. (2011). Spatial Prediction of Soil Erosion Risk by Remote Sensing, GIS and RUSLE Approach: A Case Study of Siruvani River Watershed in Attapady Valley, Kerala, India. *Environmental Earth Sciences*, 64, 965-972.
- [57]. Angima, S. D., Stott, D.E., O'Neill, M. K., Ong, C. K., & Weesies, G. A. (2003). Soil Erosion Prediction Using RUSLE for Central Kenyan Highland Conditions. *Agriculture, Ecosystem & Environment*, 97, 295-308.
- [58]. Krishna Bahadur, K. C. (2009). Mapping Soil Erosion Susceptibility Using Remote Sensing and GIS: A Case of the Upper Nam Wa Watershed, Nan Province, Thailand. *Environmental Geology*, 57, 695-705.
- [59]. López-Vicente, M., Navas, A., & Machín, J. (2008). Identifying Erosive Periods by Using RUSLE Factors in Mountain Fields of the Central Spanish Pyrenees. *Hydrology and Earth System Sciences*, 12, 523-535.
- [60]. Eltaif, N., Gharaibeh, M., Al-Zaitawi, F., & Alhamad, M. (2010). Approximation of Rainfall Erosivity Factors in North Jordan. *Pedosphere*, 20, 711-717.
- [61]. Renard, K., & Freimund, J. R. (1994). Using Monthly Precipitation Data to Estimate R-Factor in the Revised USLE. *Journal of Hydrology*, 157, 287-306.

- [62]. El-Swaify, S. A. (1997). Factors Affecting Soil Erosion Hazards and Conservation Needs for Tropical Steep Lands. *Soil Technology*, 11, 3-16.
- [63]. Phinzi, K., & Ngetar, N. S. (2018). The Assessment of Water-Borne Erosion at Catchment Level Using GIS-Based RUSLE and Remote Sensing: A Review. *International Soil and Water Conservation Research*, 7, 27-46.
- [64]. Mhangara, P., Kakembo, V., & Lim, K. J. (2012). Soil Erosion Risk Assessment of the Keiskamma Catchment, South Africa Using GIS and Remote Sensing. *Environmental Earth Sciences*, 65, 2087-2092.
- [65]. Wischmeier, W. H. (1971). A Soil Erodibility Monograph for Farmland and Construction Sites. *Journal of Soil and Water Conservation*, 26, 189-193.
- [66]. Khresat, A., Rawajfih, Z. and Mohammad, M. (1998). Land Degradation in North-Western Jordan: Causes and Processes. *Journal of Arid Environment*, 39, 623-629.
- [67]. Pradhan, B., Chaudhari, A., Adinarayana, J., & Buchroithner, M. (2012). Soil Erosion Assessment and its Correlation with Landslide Events Using Remote Sensing Data and GIS: A Case Study at Penang Island, Malaysia. *Environmental Monitoring and Assessment*, 184, 715-727.
- [68]. Bollinne, A., & Rosseau, P. (1978). The Soil Erodibility of the Medium and High Belgium, using a Method of Calculating the K Factor of the Universal Soil Loss Equation (In French). *Bulletin Société Belged'EtudesGéographiques*, 14, 127-140.
- [69]. Datta, P. S., & Schack-Kirchner, H. (2010). Erosion Relevant Topographical Parameters Derived from Different DEMs – a Comparative Study from the Indian Lesser Himalayas. *Remote Sensing*, 2, 1941-1961.
- [70]. Wu, L., Long, T., Liu, X., & Mmerek, D. (2012). Simulation of Soil Loss Processes Based on Rainfall Runoff and the Time Factor of Governance in the Jialing River Watershed, China. *Environmental Monitoring and Assessment*, 184, 3731-3748.
- [71]. Moore, I. D., & Burch, G. J. (1986a). Modeling Erosion and Deposition: Topographic Effects. *Transactions of the American Society of Agricultural Engineers*, 26, 1624-1630.
- [72]. Moore, I. D., & Burch, G. J. (1986b). Physical Basis of the Length-Slope Factor in the Universal Soil Loss Equation. *Soil Science Society of America Journal*, 50, 1294-1298.
- [73]. McCool, D. K., Foster, G. R., Renard, K. G., & Weesies, G. A. (1995). The Revised Universal Soil Loss Equation. Proceedings of DOD Interagency Workshop on Technologies to Address Soil Erosion on DOD Lands, San Antonio, Department of Defence. <https://www.tucson.ars.ag.gov/unit/publications/PDFfiles/1132.pdf>.
- [74]. Das, B., Paul, A., Bordoloi, R., Tripathi, O., & Pandey, P. K. (2018). Soil Erosion Risk Assessment of Hilly Terrain through Integrated Approach of RUSLE and Geospatial Technology: A Case Study of Tirap District, Arunachal Pradesh. *Modelling Earth System and Environment*, 4, 373-381.
- [75]. Wang, G., Went, S., Gertner, G. Z., & Anderson, A. (2002). Improvement in Mapping Vegetation Cover Factor for the Universal Soil Loss Equation by Geostatistical Methods with Landsat Thematic Mapper Images. *International Journal of Remote Sensing*, 23, 3649-3667.
- [76]. Van der Knijff, J. M., Jones, R. J. A., & Montanarella, L. (1999). Soil Erosion Risk Assessment in Italy. European Soil Bureau, Joint Research Centre of the European Commission. https://www.researchgate.net/profile/Luca_tanarella/publication/254764323_Soil_Erosion_Risk_Assessment_in_Italy/links/02e7e5352d90f8e0f9000000/Soil-Erosion-Risk-Assessment-in-Italy.pdf.
- [77]. Renard, K. G., Yoder, D. C., Lightle, D. T., & Dabney, S. M. (2011). Universal Soil Loss Equation and Revised Universal Soil Loss Equation. In: Morgan, R.P.C. and Nearing, M.A. (Eds.), *Handbook of Erosion Modelling* (pp. 137–167). Chichester: Blackwell Publishing Ltd.
- [78]. Adornado, H.A., Yoshida, M., & Apolinare, H. (2009). Erosion Vulnerability Assessment in REINA, Quezon Province, Philippines with Raster-based Tool Built within GIS Environment. *Journal of Agricultural Research*, 18, 24–31.
- [79]. Morgan, J. L., Gergel, S. E., & Coops, N. C. (2010). Aerial Photography: A Rapidly Evolving Tool for Ecological Management. *BioScience*, 60, 47-59.
- [80]. David, W.P. (1988). Soil and Water Conservation Planning: Policy Issues and Recommendations. *Philippine Journal of Development*, 14, 47-84.
- [81]. Irvem, A., Topaloglu, F., & Uyagur, V. (2007). Estimating Spatial Distribution of Soil Loss over Seyhan River Basin in Turkey. *Journal of Hydrology*, 336, 30-37.
- [82]. Ozsoy, G., Aksoy, E., Dirim, M. S., & Tumsavas, Z. (2012). Determination of Soil Erosion Risk in the MustafakemalPasa River Basin, Turkey, Using the Revised Universal Soil Loss Equation, Geographic Information System, and Remote Sensing, *Environmental Management*, 50, 679-694.
- [83]. Farhan, Y., & Al-Shaikh, N. (2017). Quantitative Regionalization of W. Mujib-Wala Sub-Watersheds (Southern Jordan) Using GIS and Multivariate Statistical Techniques. *Open Journal of Modern Hydrology*, 7, 165-199. doi: 10.4236/ojmh.2017.72010.
- [84]. Nearing, M. A., Ascough, L. D. & Laflen, J. M. (1990). Sensitivity Analysis of the WEPP Hillslope Profile Erosion Model. *Transactions of the American Society of Agricultural Engineering*, 33, 839-849.
- [85]. Bouguerra, H., Bouanani, A., Khanouch, K., Dardous, O., & Tachi, S. E. (2017). Mapping Erosion Prone Areas in the Bouhamdane Watershed (Algeria) Using the Revised Universal Soil Loss Equation through GIS. *Journal of Water and Land Development*, 32, 13-23.
- [86]. Patel, D., Gajjar, C., & Srivastara, P. (2013). Prioritization of Malesari Mini-Watersheds through Morphometric Analysis: A Remote Sensing and GIS Perspective. *Environmental Earth Sciences*, 69, 2643-2656.
- [87]. Makwana, J., & Tiwari, M. (2016). Prioritization of Agricultural Watersheds in Semi-Arid Middle Region of Gujarat Using Remote Sensing and GIS. *Environmental Earth Sciences*, 75, 137-159.
- [88]. Nooka Ratnam, K., Srivastava, Y. K., Venkateshwara Rao, V., Amminedu, E., & Murthy, K. S. R. (2005). Check Dam Positioning and Prioritization of Micro-Watersheds using SYI Model and Morphometric Analysis — Remote Sensing and GIS Perspective.

Journal of the Indian Society of Remote Sensing, 33, 25-38.

[89]. Gajbhiye, S. M., & Sharma, S. K. (2015). Prioritization of Watersheds through Morphometric Parameters: A PCA Approach. *Applied Water Science*, 7, 1505-1519.

[90]. Burdon, D. (1959). Handbook of the Geology of Jordan. Benham & Co., Colchester.

[91]. Cordova, C. E. (2000). Geomorphological Evidence of Intense Prehistoric Soil Erosion in the Highlands of Central Jordan. *Physical Geography*, 2, 538-567.

[92]. Abu-Zreig, M. M., Tamimi, A., & Alazba, A. A. (2011). Soil Erosion Control and Moisture Conservation in Arid Land with Stone Cover. *Arid Land Research and Management*, 25, 297-307.

[93]. Sharaiha, R., & Ziadat, F. (2007). Alternative Cropping Systems to Control Soil Erosion in Arid to Semi-Arid Areas of Jordan. *African Crop Science Conference Proceedings*, 8, 1559-1565.

[94]. Shammout, S. (1980). The Jordanian Experience in Rainfed Agriculture, Paper Submitted to the Rainfed Agriculture in the Near East and North Africa Meeting, FAO, Rome.

How to cite this article: Nawaiseh, S. (2020). Wadi Ziqlab Revisited: Estimation of Soil Loss and Prioritization of a Mountainous Watershed (Northern Jordan) Using RUSLE and GIS. *International Journal on Emerging Technologies*, 11(5): 658–671.